Available online at www.sciencedirect.com

ScienceDirect

Procedia Computer Science 167 (2020) 677–685

Procedia Computer Science

www.elsevier.com/locate/procedia

International Conference on Computational Intelligence and Data Science (ICCIDS 2019)

MR Image Enhancement using Adaptive Weighted Mean Filtering and Homomorphic Filtering

P. Yugander[a] , C.H. Tejaswini[a], J. Meenakshi[a], K. Samapath kumar[a], B.V.N Suresh Varma[a], M. Jagannath[b,*]

[a]*Kakatiya Institute of Technology and Science, Warangal, Telangana, India*
[b]*Vellore Institute of Technology (VIT), Chennai, Tamil Nadu, India*

Abstract

Magnetic resonance image enhancement plays crucial role in numerous bio-medical applications. In this paper, the noisy magnetic resonance (MR) brain images were enhanced using Adaptive Weighted Mean Filtering (AWMF) and homomorphic filtering. The MR images always suffer from low contrast. Homomorphic filtering is popular technique to enhance the image contrast. Homomorphic filtering works based on illumination-reflectance model. It improves the image quality by doing contrast enhancement and dynamic range compression simultaneously. In general, MR images are affected by Rician noise, salt and pepper noise and Gaussian noise. Salt and pepper noise (SPN) considerably reduce the quality of the MR images. Contrast ratio and image quality is significantly degraded in the presence of SPN. Pre-processing is required for noisy MR images before applying to homomorphic filter. Many techniques have been proposed to de-noise the salt and pepper noise such as mean, median and adaptive filters. These filters are used to eliminate low level of SPN. High level of SPN can be eliminated by AWMF. In pre-processing, the AWMF is used to denoising the noisy images. Then de-noised image is enhanced using homomorphic filter. The efficiency of the proposed method is compared with median filter (MF) and based on pixel density filter (BPDF). The simulation results show that our proposed algorithm is more efficient than existing algorithms.

Keywords: Image Enhacement; Homomorphic Filtering; Adaptive Weighted Mean Filter (AWMF); Based on Pixel Density Filter (BPDF).

*Corresponding author. Tel.: +91-9884386262; Fax: 044-3993-2555.
E-mail address: jagan.faith@gmail.com

1877-0509 © 2020 The Authors. Published by Elsevier B.V.

10.1016/j.procs.2020.03.334

1. Introduction

Brain plays important role in human body. It controls numerous complex functions of human body. Brain imaging method is extensively used for identifying diseases like paralysis, stroke, brain tumor [1], epilepsy [2] etc. MR imaging technique uses the property of nuclear magnetic resonance (NMR) to acquire the detailed brain images. NMR uses radio waves and magnetic field to get the internal structure of the brain. In general MR images corrupted with different types of noise and artifacts at the time of image acquisition. Low contrast is the major drawback of MR images. The low contrast images are not useful for medical image processing. Contrast enhancement should be required for further analysis like segmentation, registration and fusion. Doctors can easily analyze and identify the disease from enhanced images. The number of enhancement methods has been proposed like histogram equalization [3], gamma correction, thresholding, and homomorphic filtering etc. homomorphic filtering is famous technique used for image enhancement.

Homomorphic Filtering (HF) is a frequency domain filtering method. The main advantage of HF is, it increases contrast ratio and normalizes brightness simultaneously. It is used in various applications due to the above special characteristic [4], [5]. But it fails to enhance the MR images in the presence of noise. Pre-processing is required to enhance the contrast of noisy MR images. Different types of filtering techniques are available for removing spatial domain noise. Spatial domain noise can be eliminated using mean filter, median filter, averaging filter, Wiener filter, Gaussian filter, adaptive filter, min and max filters. The filter will be selected based on the quantity and type of noise exists in the image because various filters efficiently eliminate various types of noises. In general MR images are corrupted by Rician noise [6] or salt and pepper noise (SPN) [7]. Rician noise is eliminated by wavelets and SPN is eliminated by standard mean and median filters efficiently. The standard mean and median filter eliminate low level of SPN efficiently but fails to eliminate high level of SPN. The SPN exists at the minimum or maximum gray values of the image. The number of techniques has been implemented to remove high level of SPN. For example, adaptive median filtering [8], fast switching based median-mean filter [9], an adaptive weighted median filter [10], and adaptive weighted mean filter.

The outline of the paper is as follows. The adaptive weighted mean filtering is presented in Section 2, The homomorphic filtering techniques is presented in Section 3. Section 4 shows the results and discussion and finally work is concluded in Section 5.

2. Adaptive Weighted Mean Filter

High level of SPN is drastically degrades the MR image quality. This can be eliminated using adaptive weighted mean filter (AWMF). In standard mean filter window size is fixed and it is used eliminate low level of SPN noise. But AWMF uses variable window [11]. In AWMF window size is varying according to minimum and maximum pixel values in the window. Window size expanded repeatedly up to the minimum and maximum values of two successive windows are equal. If the center pixel value in the window is equal to the minimum or maximum value, then center pixel will be restored with the average weighted value of the selected window. If the center pixel value is not equal to minimum or maximum then the intensity value is unchanged. In this algorithm, original image with M x N size is represented by f, and $x_{i,j}$ represents the center pixel intensity value of coordinate (x, y). The dynamic range is given by $G_{\min} \le x_{i,j} \le G_{\max}$, corrupted image is represented by g. $G_{\max}$ and $G_{\min}$ is used to replace the corrupted pixel of image g using equation (1):

$$g_{i,j} = \begin{cases} G_{\min} \text{ with probability } a \\ G_{\max} \text{ with probability } b \\ f_{i,j} \text{ with probability } 1-a-b \end{cases} \tag{1}$$

Noise level in the image is defined as: $c = a + b$;

The basic principle of AWMF is to suppress the false error detection and restore the corrupted pixels by weighted mean value of the selected window. Weighted mean value of selected window is given by equation (2),

$$R_{i,j}^{mean}(w)=\begin{cases}\dfrac{\sum_{k,l\in R_{i,j}(n)} p_{k,l}*g_{k,l}}{\sum_{(k,l)\in R_{i,j}(w)} p_{k,l}}, & \sum_{(k,l)\in R_{i,j}(w)} p_{k,l}\neq 0\\ -1 & Otherwise\end{cases} \tag{2}$$

Where $R_{i,j}^{mean}(w)$ weighted mean of selected window and the weight $p_{k,l}$ is set as in equation (3):

$$p_{k,l}=\begin{cases}1 & R_{i,j}^{\min}(w)<g_{k,l}<R_{i,j}^{\max}(w)\\ 0 & Otherwise\end{cases} \tag{3}$$

15	89	98	67	54	56	43	23
13	255	181	180	150	140	141	123
14	15	180	120	255	34	111	76
15	15	180	**16**	127	56	12	56
45	77	0	232	120	45	9	56
23	45	89	98	110	111	43	34
56	56	32	23	231	45	23	45

Fig.1. A window case (center pixel output using BPDF is 150 and using AWMF output 16 (unchanged)).

A noisy sub image with 8x8 size is considered for analyzing based on pixel density function (BPDF) and AWMF. Figure 1 shows noisy 8x8 sub image. Assume that *g* is a noisy 8x8 sub image. Let us assume center pixel $x(40,50) = 16$ and the window size is 3x3. In BPDF algorithm selected window checks for at least one noisy pixel and one noise free pixel [12]. SPN noise values are always either 0 or 255. In 3x3 window $x(39,51)$ contains pixel value 255 and $x(41,50)$ contains pixel value 232. Both conditions of BPDF are satisfied. If both conditions are satisfied, then center pixel $x(40,50)$ is treated as noisy pixel and this is replaced with the 150. (Center pixel is replaced with average value of the repeated pixels in the window i.e., (180+120)/2=150). Unfortunately $x(40,50) \neq$ 255 or 0. $x(40,50) = 16$ which is not equal to 255 or 0. But using BPDF algorithm noise free pixel treated as noisy pixel and 16 replace with 150, which leads to false error detection. This type of false error detection is eliminated in AWMF.

In AWMF variable window size is predicted by repeatedly increasing the window size up to the minimum and maximum pixel values of two consecutive windows are equal. In first case, a 3x3 window with center pixel $x(40,50)$ =16 is considered. For the selected 3x3 window lowest intensity value is '0' and highest intensity value is 255. After increasing window size to 5x5, lowest intensity value is 0 and highest intensity value is 255. In Fig.1 both 3x3 and 5x5 windows minimum and maximum pixel values are same. Since center pixel 16 is not equal to 0 or 255, so it can be treated as noise free pixel and the center pixel value is unchanged. But in case of BPDF noise free center pixel treated as noisy pixel and pixel value is replaced unnecessarily. This will not happen in case of AWMF. If the pixel is noisy then it will be restored by weighted average of the selected window otherwise original pixel values is unchanged.

3. Homomorphic Filtering

Homomorphic filtering is a well-known technique for enhancing low contrast medical images [14], [15]. HF works based on the illumination-reflectance model (IRM). The IRM image can be divided into two components as shown in equation (4):

$$f(x,y) = f_i(x,y).f_r(x,y)$$

(4)

$f_i(x,y)$ is illumination component and the $f_r(x,y)$ is reflectance component. The quantity of energy incident on the image is called as the illumination. The reflected amount of the object in the scene is called reflectance. The range of illumination component is $0<i(x,y)<\infty$ and reflectance component range is $0<r(x,y)<1$. Illumination components treated as low frequency components because quantity of illuminance does not change over the range. Reflectance component values changes much over the range. It is considered as high frequency component [16]. In spatial domain Illumination corresponds to smoothing and reflectance indicates edges and boundaries. Illumination and reflectance components are separated by applying logarithmic transformation. Mathematically it can be written as

$$\ln\{f(x,y)\} = \ln\{f_i(x,y).f_r(x,y)\} \tag{5}$$

Above equation (5) is simplified as shown in equation (6):

$$\ln\{f(x,y)\} = \ln\{f_i(x,y)\} + \ln\{f_r(x,y)\} \tag{6}$$

Fourier transform is applied for processing images in frequency domain,

$$FT\{\ln\{f(x,y)\}\} = FT\{\ln\{f_i(x,y)\}\} + FT\{\ln\{f_r(x,y)\}\} \tag{7}$$

Above equation (7) can be simplified as equation (8):

$$F(u,v) = F_i(u,v) + F_r(u,v) \tag{8}$$

Where $F_i(u,v) = FT\{\ln\{f_i(x,y)\}$ and $F_r(u,v) = FT\{\ln\{f_r(x,y)\}$

Filtered output in frequency domain is given by equation (9) as:

$$S(u,v) = H(u,v)F(u,v) \tag{9}$$

Where $S(u,v)$ is frequency domain filtered output, $H(u,v)$is filter response in frequency domain, and $F(u,v)$ is frequency domain image.

Above equation (9) can be simplified as equation (10):

$$S(u,v) = H(u,v)F_i(u,v) + H(u,v)F_r(u,v) \tag{10}$$

Selection of filter plays vital role in HF. In order to diagnosis the low contrast MR images contrast enhancement is required i.e., boosting of high frequencies and suppression of low frequencies are required. A high pass filter is suitable for MR image contrast enhancement. Gaussian high pass filter has been chosen for the above purpose. It is defined by equation (11):

$$H(u,v) = (f_h - f_L)\left[1 - e\left\{-c\left(\frac{D(u,v)}{D_0}\right)^2\right\}\right] + f_L \tag{11}$$

Where c is used to control the slope, f_H is the high frequency gain, f_L is the low frequency gain, $D(u,v)$ is the distance between (0,0) and coordinates (u,v), and D_0 is the cut off frequency. After the high pass filtering inverse Fourier transform is applied to get spatial domain image as in equation (12):

$$IFT\{S(u,v)\} = IFT\{H(u,v)f_i(u,v)\} + IFT\{H(u,v)f_r(u,v)\} \tag{12}$$

Above equation (12) can be simplified as in equation (13):

$$\ln\{s(x,y)\} = \ln\{g_i(u,v)\} + \ln\{g_r(u,v)\} \tag{13}$$

Where $g_i(u,v)$ and $g_r(u,v)$ are modified illumination and reflection components. Finally, exponential is applied to reconstruct the enhanced image as in equation (14):

$$g(x,y) = \exp^{\{\ln(s(x,y)=\ln\{g_i(u,v)\}+\ln\{g_r(u,v)\}\}} \tag{14}$$

Contrast enhanced image $g(x,y)$ is given by equation (15):

$$g(x,y) = g_i(x,y).g_r(x,y) \tag{15}$$

3.1. Proposed Algorithm:

Step 1: De-noise the noisy image using AWMF.
Step 2: Apply logarithmic transform to separate illumination and reflectance components.
Step 3: Convert spatial domain image into frequency domain using Fourier transform.
Step 4: Apply Gaussian high pass filter to improve the image contrast.
Step 5: Covert frequency domain image into spatial domain using inverse Fourier transform.
Step 6: Apply exponential to reconstruct contrast enhance image.

Many numbers of algorithms have been proposed to enhance the contrast of the noisy MR images. The existing techniques work with only low level of noise. Thus, the proposed algorithm is attempted to work with low level of noise as well as high level of noise.

4. Results and Discussion

Three MR images have been collected from open access series of imaging studies (OASIS) dataset (with size 256x256, 290x280, 512x512) to evaluate the performance of the proposed algorithm. Also, Performance of the proposed algorithm compared with MF and BPDF algorithms. The simulated results are shown in Fig. 2, Fig. 3 and Fig. 4. The input images are shown in Fig. 2(a), Fig. 3(a), and Fig. 4(a). The 50% SPN corrupted images are shown in Fig. 2(b) and Fig. 3(b). The 90% SPN corrupted image is shown in Fig. 4(b). In first step image is de-noised using MF. The de-noising images using MF are shown in Fig. 2(c), Fig. 3(c) and Fig. 4(c). The contrast enhancement has been done after de-noising noisy images. The de-noised images are applied to homomorphic filter for contrast enhancing. The contrast enhanced images using HF shown in Fig. 2(d), Fig. 3(d) and Fig. 4(d). The BPDF de-noised images are shown in Fig. 2(e), Fig. 3(e) and Fig. 4(e). The contrast enhanced BPDF based images are shown in Fig. 2(f), Fig. 3(f) and Fig. 4(f). Finally, AWMF is applied for image denoising. AWMF de-noised images are shown in Fig. 2(g), Fig. 3(g) and Fig. 4(g). The contrast enhanced AWMF images are shown in Fig. 2(h), Fig. 3(h) and Fig. 4(h). The results have been shown that the AWMF de-noised images effectively enhanced contrast compared to MF and BPDF de-noised images.

Three parameters such as peak signal-to-noise ratio (PSNR), signal to noise ratio (SNR) and mean square error (MSE) have been selected for evaluating the performance of proposed algorithm. The comparison results for three algorithms for different noise levels are presented in Table 1.

$$MSE = \frac{1}{MN}\sum_{m=1}^{M}\sum_{n=1}^{N}[f(x,y)-\hat{f}(x,y)]^2 \tag{16}$$

$$SNR = \frac{\sum_{x=0}^{M-1}\sum_{y=0}^{N-1}\hat{f}(x,y)}{\sum_{x=0}^{M-1}\sum_{y=0}^{N-1}[f(x,y)-\hat{f}(x,y)]^2} \tag{17}$$

$$PSNR = 10\log_{10}\left(\frac{Max^2}{MSE}\right) \tag{18}$$

Table 1 shows the MSE, SNR and PSNR for different images with various high levels of SPN. The MSE values of the AWMF are very low compare to MF and BPDF. All the three filters perform almost same for the low level of SPN noise. MF and BPDF fails to de-noise the high level SPN. For all the three images, the SNR values of AWMF are high compare to MF and BPDF. PSNR values of the MF are very low compared to BPDF and AWMF. PSNR value of the 90% corrupted mri1 image is 56.0624 dB. For the same image PSNR values of MF and BPDF are 53.0897 dB and 56.0448 dB respectively. The results were simulated using on windows 7, Intel Corei3-3110,CPU@2.40 GHz Computer. MATLAB2013a software is used to test the algorithms. Table 1 demonstrates that

AWMF performs better than other algorithms

Table 1. Comparison of MF, BPDF and AWMF filters with different noise levels

Image	Filter	Parameter	10%	20%	30%	40%	50%	60%	70%	80%	90%
		MSE	0.1625	0.1630	0.1676	0.1780	0.1963	0.2250	0.2573	0.2929	0.3217
	MF	SNR	12.5987	12.5731	12.3305	11.8068	10.9595	9.7711	8.6072	7.4821	6.6663
		PSNR	56.0559	56.0431	55.9218	55.6599	55.2363	54.6421	54.0601	53.4976	53.0897
		MSE	0.1990	0.2294	0.2566	0.2770	0.2888	0.2855	0.2648	0.2240	0.1620
MRI1	**BPDF**	SNR	10.7913	9.5546	8.6317	7.9192	7.5548	7.6558	8.3078	9.7617	12.5765
		PSNR	55.1768	54.5585	54.0724	53.7407	53.5586	53.6090	53.9350	54.6620	56.0448
		MSE	0.1640	0.1635	0.1629	0.1623	0.1621	0.1625	0.1628	0.1625	0.1633
	AWMF	SNR	12.4461	12.4745	12.5032	12.5354	12.5493	12.5265	12.4867	12.5239	12.3581
		PSNR	56.0165	56.0308	56.0451	56.0612	56.0681	56.0568	56.0493	56.0555	56.0624
		MSE	0.1210	0.1224	0.1284	0.1459	0.1755	0.2145	0.2578	0.2961	0.3268
	MF	SNR	15.1617	15.0582	14.6474	13.5348	11.9319	10.1890	8.5900	7.3867	6.5316
		PSNR	57.3374	57.2856	57.0802	56.5239	55.7225	54.8510	54.0515	53.4499	53.0224
		MSE	0.1946	0.2343	0.2686	0.2973	0.3126	0.3085	0.2804	0.2329	0.1651
MRI2	**BPDF**	SNR	11.0332	9.3733	8.2342	7.3024	6.9169	6.9833	7.8606	9.4224	12.4135
		PSNR	55.2731	54.4678	53.8736	53.4323	53.2150	53.2728	53.6868	54.4923	55.9879
		MSE	0.1215	0.1212	0.1208	0.1207	0.1208	0.1206	0.1207	0.1198	0.1215
	AWMF	SNR	13.9828	13.9986	14.0318	13.9138	14.0315	13.9247	13.5597	13.9761	13.8878
		PSNR	57.3203	57.3282	57.3448	57.3473	57.3447	57.3528	57.3471	57.3785	57.3189
		MSE	0.1841	0.1848	0.1887	0.1986	0.2179	0.2429	0.2758	0.3060	0.3303
	MF	SNR	11.5144	11.4831	11.3026	10.8575	10.0501	9.1091	8.0036	7.1018	6.4396
		PSNR	55.5137	55.4981	55.4079	55.1853	54.7816	54.3111	53.7584	53.3074	52.9763
		MSE	0.2869	0.2411	0.2151	0.1988	0.1797	0.1598	0.1377	0.1103	0.0789
MRI3	**BPDF**	SNR	7.6138	9.1727	10.1629	10.8478	11.6787	12.6970	13.9883	15.9664	18.8257
		PSNR	53.5881	54.3429	54.8380	55.1805	55.6205	56.1297	56.7753	57.7398	59.1940
		MSE	0.1781	0.1783	0.1781	0.1781	0.1783	0.1779	0.1779	0.1773	0.1812
	AWMF	SNR	11.7802	11.7696	11.7797	11.7774	11.7688	11.7899	11.7866	11.8163	11.6285
		PSNR	55.6590	55.6536	55.6587	55.6575	55.6533	55.6638	55.6621	55.6770	55.5831

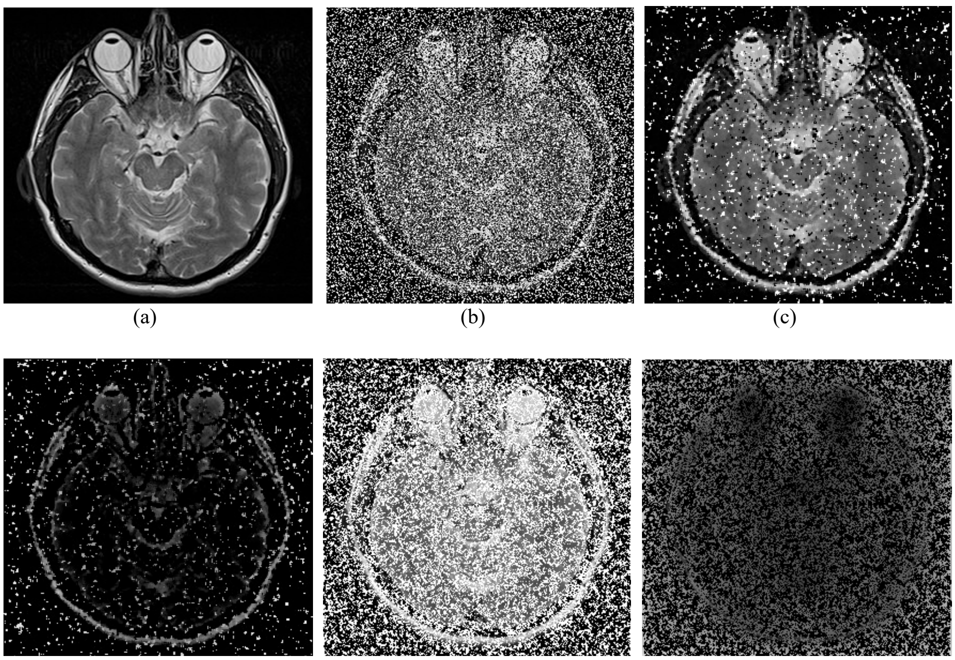

(a) (b) (c)

(d) (e) (f)

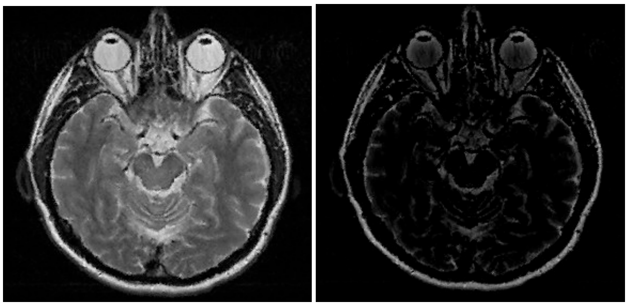

(g) (h)

Fig.2. (a) Input image (290x280) (b) Noisy image with 50% SPN (c) De-noised image using MF (d) Homomorphic filtered output (e) Denoised image using BPDF (f) Homomorphic filtered output (g) De-noised image using AWMF (h) Homomorphic filtered output

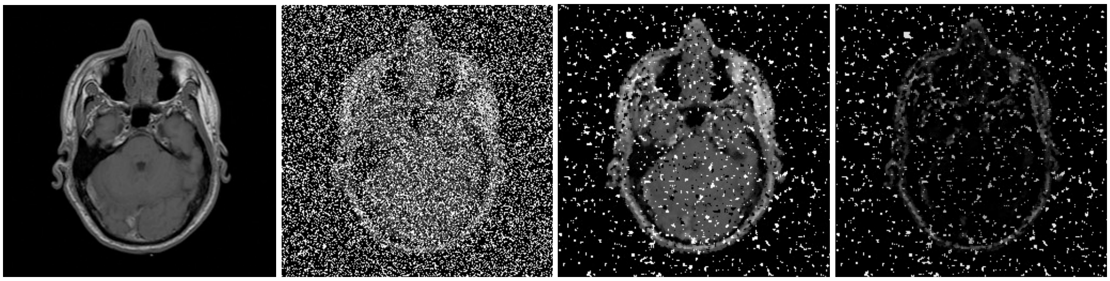

(a) (b) (c) (d)

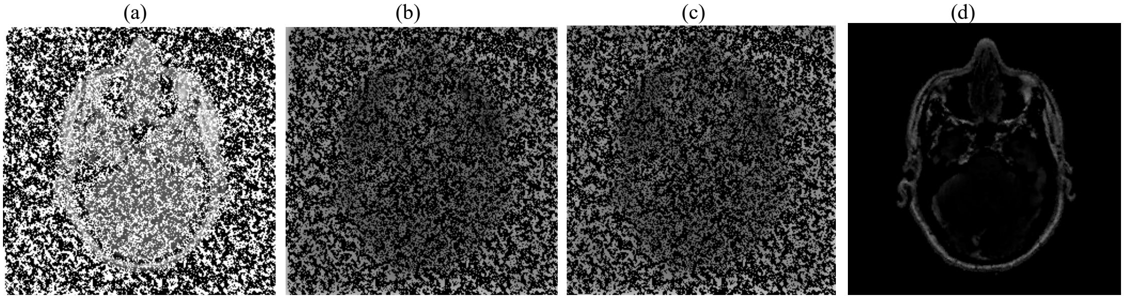

(e) (f) (g) (h)

Fig.3. (a) Input image (256x256) (b) Noisy image with 50% SPN (c) De-noised image using MF (d) Homomorphic filtered output (e) Denoised image using BPDF (f) Homomorphic filtered output (g) De-noised image using AWMF (h) Homomorphic filtered output

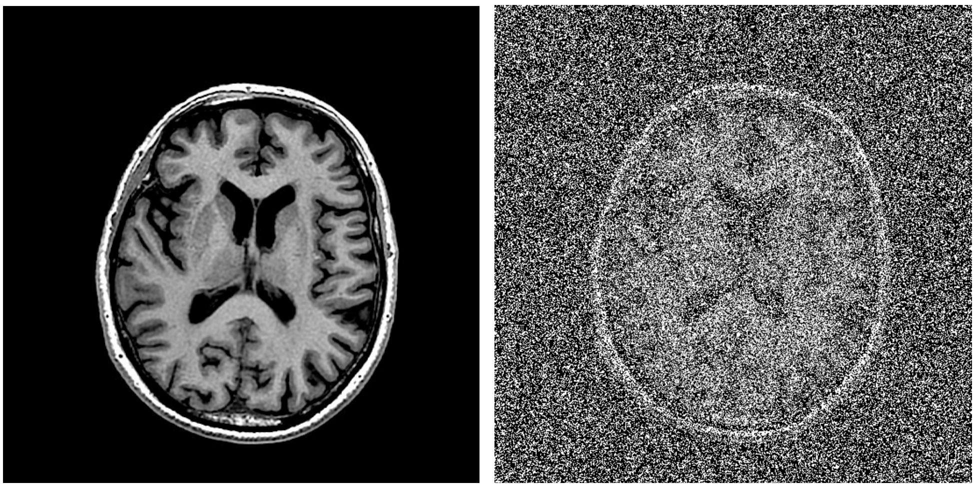

(a) (b)

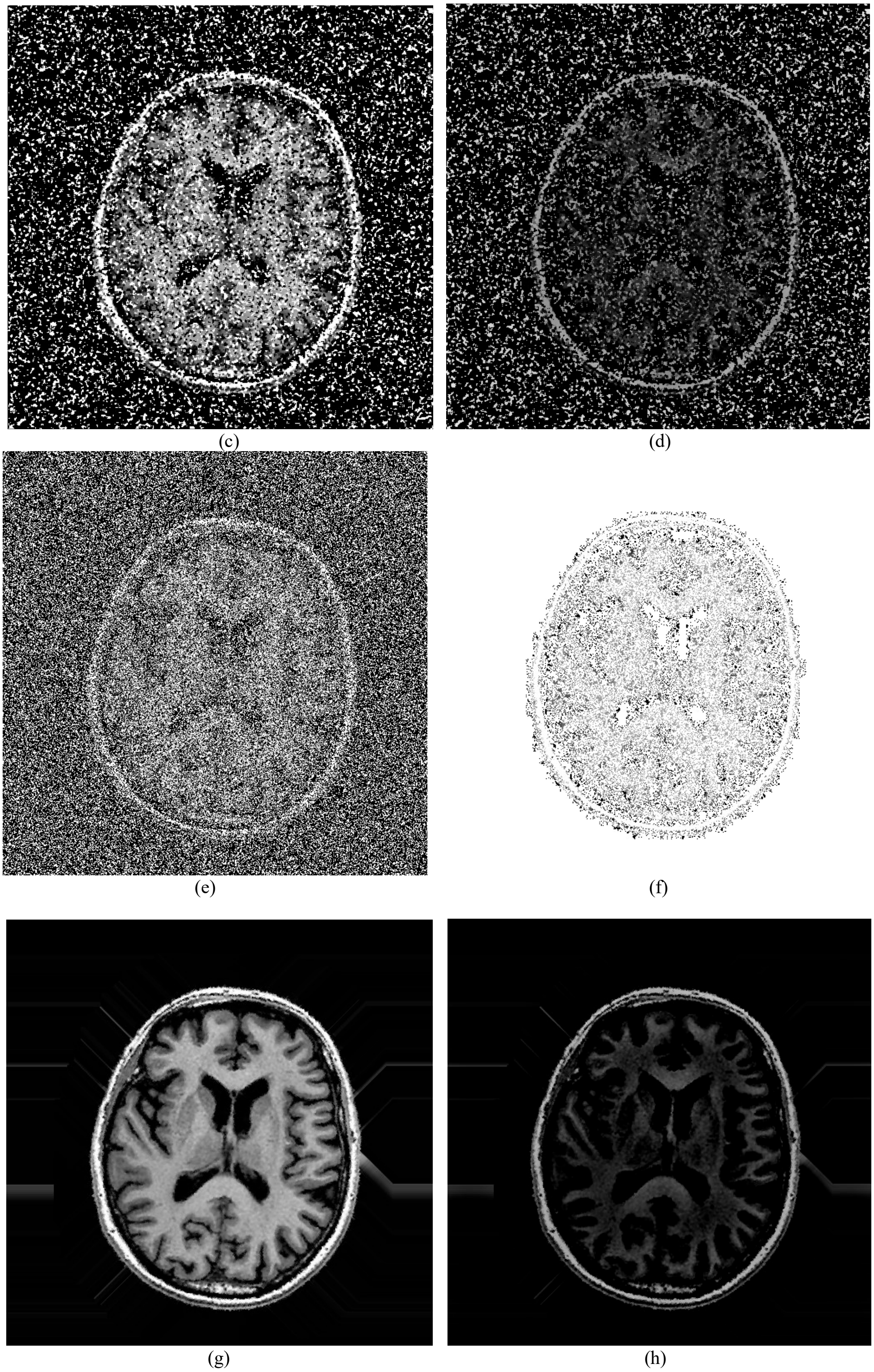

Fig.4. (a) Input image (512x512) (b) Noisy image with 70% SPN (c) De-noised image using MF (d) Homomorphic filtered output (e) Denoised image using BPDF (f) Homomorphic filtered output (g) De-noised image using AWMF (h) Homomorphic filtered output

4. Conclusion

In this paper a novel algorithm for MR image contrast enchantment is proposed and tested on noisy MR images. The main drawback of MR image is low contrast. Researchers have been proposed number of enhancement algorithms. HF is the most popular algorithm for contrast enhancement. Unfortunately, HF fails to enhance the MR images in the presence of noise. Pre-processing is required for noisy images. Most of the algorithms work efficiently under noise free condition. Basically, MR images corrupted with RN and SPN at the time of data acquisition. Standard mean and median filters eliminate low level of SPN. The high level SPN cannot be eliminated by standard filters. The high level SPN can be eliminated by using AWMF algorithm. The three images from OASIS dataset have been collected for testing and validating the proposed and existing algorithms. The performance of the AWMF is tested with two more existing algorithms. Three noisy MR images are used to test the MF, BPDF and AWMF algorithms. Three algorithm performances have been tested using MSE, SNR and PSNR. Results have been proven that the AWMF performs well compare to MF and BPDF. In this paper, the proposed algorithm is applied to 2D structural MR images only. The proposed algorithm can be extended to 3D MR Images and diffusion tensor images.

References

[1] Kimura M, and da Cruz L.C.H. (2016) "Multiparametric MR imaging in the assessment of brain tumors." *Magnetic Resonance Imaging Clinics of North America* **24 (1)**: 87-122.

[2] Peng B, Wu and Chen Y. (2015) "Volumetric changes in amygdala and entorhinal cortex and their relation to memory impairment in patients with medical temporal lobe epilepsy with visually normal MR imaging findings." *Epilepsy Research* **114**: 66-72.

[3] Agarwal M and Mahajan R. (2018) "Medical image contrast enhancement using range limited weighed histogram equalization." *Procedia of Computer Science* **125**: 149-156.

[4] Xiao L, Wu Z and Wang T. (2016) "An enhancement method for X-ray image via fuzzy noise removal and homomorphic filtering." *Neurocomputing* **195**: 56-64.

[5] Fan C and Zhang. (2011) "Homomorphic filtering-based illumination normalization method for face recognition." *Pattern Recognition Letters* **32 (10)**: 1468-1479.

[6] Coupe P, Manjon J V. (2010) "Robust Rician noise estimation for MR images." *Medical Image Analysis* **14 (4)**: 483-493.

[7] Hanafy M. (2016) "A new method to remove salt and pepper noise in magnetic resonance images." *In Proceedings of the International Conference on Computer Engineering & Systems.*" 155-160.

[8] Yuan S Q and Tan Y. (2006) "Impulse noise removal by a global-local noise detector and adaptive median filter." *Signal Processing* **86 (8)**: 2123-2128.

[9] Vijaykumar V.R and Santhana M.G, and Ebenezer D. (2014) "Fast switching based median-mean filter for high density salt and pepper noise removal." *AEU-International Journal of Electronics and Communications* **68 (12)**:1145-1155.

[10] T. Loupas, W.N McDicken, andP.L. Allan. (1989) "An adaptive weighted median filter for speckle suppression in medical ultrasonic images." *IEEE Transactions on Circuits and Systems* **36 (1)**: 129-135.

[11] Zhang P and Fang Li. (2014) "A new adaptive weighted mean filter for removing salt and pepper noise." *IEEE Signal Processing Letters* **21(10)**: 1280-1283.

[12] Erkan U and Gokrem L. (2018) "A new method based on pixel density in salt and pepper noise removal." *Turkish Journal of Electrical Engineering and Computer Sciences* **26 (1)**: 162-171.

[13] Brinkamann B.H, Manduca, and Robb R.A. (1998) "Optimized homomorphic unsharp masking for MR gray scale inhomogeneity correction." *IEEE Transactions on Medical Imaging* **17 (2)**: 161-171.

[14] Karthik R.S, Havlicek M and Gopikrishna D. (1995) "Nonparametric hemodynamic deconvolution of fMRI using homomorphic filtering." *IEEE Transaction on Medical Imaging* **34 (5)**: 1122-1163.

[15] Daniel E. (2006) "Optimum wavelet-based homomorphic medical image fusion using hybrid genetic-grey wolf optimization algorithm." *IEEE Sensor Journal* **18 (16)**: 6804-6811.

[16] Aswathy M.A, and Jagannath M. (2016) "Detection of breast cancer on digital histopathology images: present status and future possibilities." *Informatics in Medicine Unlocked* **8**: 74-79.